UWA Massive MIMO Communications

Amir Aminjavaheri and Behrouz Farhang-Boroujeny
ECE Department, University of Utah, Salt Lake City

***Abstract*—Underwater acoustic (UWA) channels are characterized by low availability of bandwidth, large propagation delays and fast varying multipaths. The fast variation of multipaths, in particular, hampers the bandwidth efficiency of UWA channels, as a significant percentage of transmission resources should be allocated to pilots. The problem magnifies further in the case of multiple-input multiple-output (MIMO) channels as the number of pilots increases linearly with the number of transmitting transducers. This paper introduces the concept of massive MIMO (a technology that has recently been proposed as a candidate for 5G wireless communication systems) for UWA channels and shows that the choice of filter bank multicarrier (FBMC) modulation for transmission in a multicarrier system removes the need for pilots, hence achieves a high level of bandwidth efficiency.**

I. Introduction

Multiple-input multiple-output (MIMO) technology has emerged in the recent past as a unique solution for increasing the throughput and reliability of wireless communication systems. MIMO technology have been successfully applied to both the traditional electromagnetic wireless channels and the underwater acoustic (UWA) communications. Point-to-point MIMO systems incorporate multiple antennas at both sides of the communication link and thus can benefit from the additional dimension of space. This, however, requires expensive multi-antenna terminals. Moreover, multiplexing gains may not be satisfactory in the low signal-to-noise (SNR) regime or in line-of-sight (LOS) conditions where the signals from different antennas cannot be resolved.

As an alternative to point-to-point MIMO, multiuser-MIMO (MU-MIMO) has been suggested to increase the network capacity, [1]. In this case, the mobile terminals can be cheap single-antenna devices that are separated from each other by tens or hundreds of wavelengths, and the multiplexing gains are shared between them. A base station (BS) with multiple antennas is considered to be at the other end of this communication scenario.

Built upon the MIMO technology, *Massive MIMO* has been recently suggested to further improve the throughput and reliability of wireless communication systems, [2]. Massive MIMO, in essence, considers a MU-MIMO system which incorporates a BS with a large number of antennas; an order of magnitude larger than the number of users that it serves. It is proven mathematically that the effect of uncorrelated noise and multiuser interference will vanish as the number of BS antennas grows [2]. This has initiated a broad range of research studies that seriously consider Massive MIMO as a strong candidate for the 5^{th} generation of wireless cellular systems, 5G, [3].

In this paper, the application of Massive MIMO to UWA communications is advocated. Massive MIMO, when applied to UWA communications, brings a number of benefits, and the goal of this paper is to highlight these benefits. To this end, we note that all UWA channels share the following features, [4]:

1) fast variation in time; equivalently, wide dispersion in frequency,
2) wide dispersion in time, and
3) limited spectral resources.

Moreover, because of 1) and 2), UWA channels are said to be *doubly dispersive*.

Obviously, any design of a communication system for UWA channels should take the above features into account. For instance, if OFDM (orthogonal frequency division multiplexing) is adopted, a long symbol guard interval (cyclic prefix or zero padding) is required to take care of the extended impulse response of the UWA channels. But, with a long symbol guard interval, the duration of each OFDM symbol should also be made long (a few times longer than the guard interval length) to keep a good bandwidth efficiency. But, such a choice may contradict the fast variation of UWA channels in time which dictates the use of shorter OFDM symbols. This point was recently brought up in [5], where the authors proposed a special filter bank multicarrier (FBMC) waveform that was designed to cope with the doubly dispersive nature of UWA channels.

The limited spectral resources in UWA channels, on the other hand, has often been hampered by allocating a large portion of the spectral resources to pilot symbols. Such allocation deemed necessary to cope with the doubly dispersive nature of UWA channels.

This paper, beside introducing the application of Massive MIMO to UWA communications, discusses a special form of FBMC system (different from the one proposed in [5]). Overall, our design offers the following advantages. i) By increasing the number of BS antennas in a MIMO-FBMC system, the symbol duration may be decreased by almost an order of magnitude when compared to those of the previous reports on OFDM, e.g., [6], as well as the one considered in [5]. The choice of short symbol duration enables us to track the channel variations adaptively using blind techniques. ii) FBMC offers a blind equalization method that allows complete removal of pilot symbols, hence, improves the bandwidth efficiency of transmission. Only a preamble training symbol is used to initialize the equalizers. During the payload the blind equalization algorithm tracks channel variations. iii) Our simulation studies show that we are able to transmit 8

This work has been supported by National Science Foundation under award numbers 1102115.

978-0-933957-43-5 ©2015 MTS

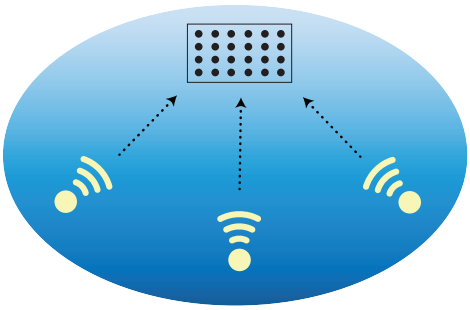

Fig. 1: UWA Massive MIMO network.

bits of coded information per second per Hertz when four independent nodes/sensors transmit to a BS/fusion center, simultaneously.

The rest of this paper is organized as follows. Section II discusses the scenario that this paper is aiming to build a network based on. Section III provides an overview of different FBMC methods that have been proposed in the past. Details of the FBMC waveform that is adopted in this paper is explained in Section IV. Section V contains the details of our Massive MIMO design. Various aspects of our design are analyzed through numerical simulations in Section VI, and finally, concluding remarks are drawn in Section VII.

II. Scenario

The MU-MIMO setup that we consider in this paper is depicted in Fig. 1. At the center of this network, there is a UWA BS with a large number of receiving hydrophones. Each transmitting node is equipped with a single loudspeaker. The BS array can be either linear, rectangular, or any other form. But, in order to provide sufficient space resolution, it is important that the spacing between the antenna elements be larger than half of the wavelength. Assuming a center frequency of $f_c = 15$ kHz, and the acoustic wave propagation speed of $c = 1500$ m/s, the minimum antenna spacing can be calculated as $0.5\lambda = 0.5 \times 1500/15000 = 5$ cm. An example of this scenario might be an underwater sensor network, where the sensor nodes are transmitting their measurements to a fusion center.

III. FBMC Methods

The first proposal on FBMC technique came from Chang, [7], who presented the conditions required for signaling a parallel set of pulse amplitude modulated (PAM) symbol sequences through a bank of overlapping filters. Saltzberg, [8], extended the idea and showed how the Chang's method could be modified for transmission of quadrature amplitude modulated (QAM) symbols. In the literature, this method is often referred to as offset-QAM (OQAM) OFDM. Efficient digital implementation of Saltzberg's multicarrier system through polyphase structures was first studied by Hirosaki [9], and was further developed by others, e.g., [10]–[12].

The pioneering work of Chang, [7], on the other hand, has received less attention within the signal processing community. Those who have cited [7], have only acknowledged its existence without presenting much details, e.g., [11]. However, the cosine modulated filter banks that have been widely studied within the signal processing community, [13], are nothing but a reinvention of Chang's filter bank, formulated in discrete-time. The use of cosine modulated filter banks for data transmission was first presented in [14] and further studied in [15], under the name discrete wavelet multitone (DWMT). Many other researchers subsequently studied and evaluated DWMT; see [16] and the references therein. Moreover, [16] suggested a blind equalization method for cosine modulated based/DWMT systems. An analysis of this blind equalizer was later developed in [17]. The name cosine modulated multitone (CMT), that we use in the rest of this paper, to refer to the Chang's type of multicarrier modulation was also coined in [17]. Another relevant work is [18], where the authors have shown that CMT and OQAM-OFDM are related through a trivial modulation step.

It is worth mentioning that, although CMT is adopted in this paper, all of the discussions and developments are applicable to the case of OQAM-OFDM as well.

IV. The CMT Waveform

In CMT, a set of real-valued data symbols are modulated and placed at different subcarriers. Moreover, to maintain the orthogonality of the data symbols at the receiver, the carrier phases are toggled between 0 and $\pi/2$ among adjacent symbols in time and frequency. This results in a time-frequency lattice structure as depicted in Fig. 2. Furthermore, the subcarriers are filtered using a time and frequency well-localized prototype filter. The subcarrier localization of FBMC is a key property that makes it robust to interferences in multiuser networks [19]. The transmitted CMT signal can be represented as [20]

$$x(t) = \sum_{n=-\infty}^{+\infty} \sum_{k=0}^{M-1} s_{n,k} \underbrace{e^{j\phi_{n,k}} g(t-nT) e^{j\frac{(2k+1)\pi}{2T}t}}_{g_{n,k}(t)}, \qquad (1)$$

where $s_{n,k}$ is the real-valued data symbol at the (n,k) time-frequency point, $\phi_{n,k} = \frac{\pi}{2}(n+k)$ is the phase-adjustment term, $g(t)$ is a square-root Nyquist prototype filter, which is well-localized in time and frequency, T denotes the symbol spacing, and M is the number of subcarriers. In (1), the terms $g_{n,k}(t)$ can be thought as a set of basis functions that are used to modulate the data symbols. In this way, the data symbols can be demodulated at the receiver free of interference if the basis functions are orthogonal. Here, since the data symbols are real-valued numbers, orthogonality in the real field should be considered:

$$\Re\left\{\int_{-\infty}^{+\infty} g_{n_1,k_1}(t) g^*_{n_2,k_2}(t) dt\right\} = \delta_{n_1,n_2}\delta_{k_1,k_2}, \qquad (2)$$

where $\Re\{\cdot\}$ denotes the real-part of a complex number, the superscript $*$ indicates complex conjugation, and δ_{n_1,n_2} is the Kronecker delta function.

When the transmitted signal is distorted by a fading time-dispersive channel, $h(\tau,t)$, it is commonly assumed that the channel is approximately constant over the length of the prototype filter, $g(t)$ and is approximately frequency flat over the

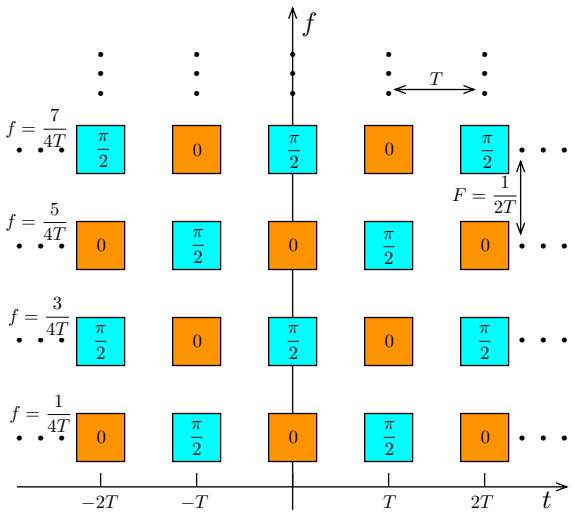

Fig. 2: The time-frequency placement of symbols in a CMT system. Each symbol is also filtered using a time-frequency localized prototype filter.

with of each subcarrier. Considering the above assumptions, the demodulated symbol can be written as, [21],

$$y_{n,k} = h_{n,k}(s_{n,k} + j \underbrace{\sum_{(p,q)\in\Omega_{n,k}} \sum G_{p,q}^{n,k} s_{p,q}}_{q_{n,k}}) + v_{n,k}. \tag{3}$$

Here, $h_{n,k}$ is the channel frequency response at the center of k^{th} subcarrier and n^{th} symbol time, $G_{p,q}^{n,k} = \Im\{\int_{-\infty}^{+\infty} g_{p,q}(t) g_{n,k}^*(t) dt\}$ is the imaginary part of the inner product between the basis functions, $\Omega_{n,k}$ denotes the set of immediate time-frequency neighborhood points of (n,k) where the inner product $G_{p,q}^{n,k}$ is non-negligible and $v_{n,k}$ is the frequency domain noise.

According to (3), the real-valued CMT symbols are subject to an imaginary interference, $q_{n,k}$, which is known as *intrinsic interference*. We can also think of (3) as if the complex-valued effective symbol $x_{n,k} = s_{n,k} + jq_{n,k}$, has been transmitted and is scaled by the gain of the channel, $h_{n,k}$. Accordingly, after the demodulation process, we can equalize the effect of the channel by applying the scaling factor $w_{n,k}^* = 1/h_{n,k}$ and taking a real-part of the result. In order to make the derivations of the subsequent sections easier to follow, we express (3) in matrix form as

$$\begin{bmatrix} y_{n,k}^{\text{R}} \\ y_{n,k}^{\text{I}} \end{bmatrix} = \begin{bmatrix} h_{n,k}^{\text{R}} & -h_{n,k}^{\text{I}} \\ h_{n,k}^{\text{I}} & h_{n,k}^{\text{R}} \end{bmatrix} \begin{bmatrix} s_{n,k} \\ q_{n,k} \end{bmatrix} + \begin{bmatrix} v_{n,k}^{\text{R}} \\ v_{n,k}^{\text{I}} \end{bmatrix}, \tag{4}$$

where the superscripts 'R' and 'I' denote the real and imaginary parts, respectively.

V. UWA Massive MIMO Design

In this section, the single-input-single-output derivations of Section IV are extended to the MU-MIMO case. Our first results in Section V-A are similar to those in [2], which confirm the merits of Massive MIMO, in general. The applicability of Massive MIMO to UWA channels, and the explanation of why this approach is advantageous follows afterwards.

A. Effect of Large Number of BS Antennas

A MU-MIMO scenario, as discussed in Section II, is considered. There exist K users which are served simultaneously by a BS consisting of N hydrophones. It is assumed that $N \gg K$. For simplicity of formulations, the time and subcarrier indices are ignored throughout this section. Accordingly, we define the vector of symbols of different users as $\mathbf{s} = [s_0, \ldots, s_{K-1}]^{\text{T}}$, the vector of corresponding intrinsic interferences as $\mathbf{q} = [q_0, \ldots, q_{K-1}]^{\text{T}}$, the vector of channel gains from the ℓ^{th} user to the BS antennas as $\mathbf{h}(\ell) = [h_{\ell,0}, \ldots, h_{\ell,N-1}]^{\text{T}}$, the matrix of channel gains as $\mathbf{H} = [\mathbf{h}(0), \ldots, \mathbf{h}(K-1)]$, the vector of noise contributions as $\mathbf{v} = [v_0, \ldots, v_{N-1}]^{\text{T}}$ and the vector of demodulated symbols at the BS antennas as $\mathbf{y} = [y_0, \ldots, y_{N-1}]^{\text{T}}$. Here, the superscript 'T' denotes the matrix transpose. Following the above definitions, extension of (4) to the case of MU-MIMO is straightforward, and the result is

$$\underbrace{\begin{bmatrix} \mathbf{y}^{\text{R}} \\ \mathbf{y}^{\text{I}} \end{bmatrix}}_{\widetilde{\mathbf{y}}} = \underbrace{\begin{bmatrix} \mathbf{H}^{\text{R}} & -\mathbf{H}^{\text{I}} \\ \mathbf{H}^{\text{I}} & \mathbf{H}^{\text{R}} \end{bmatrix}}_{\widetilde{\mathbf{H}}} \underbrace{\begin{bmatrix} \mathbf{s} \\ \mathbf{q} \end{bmatrix}}_{\widetilde{\mathbf{x}}} + \underbrace{\begin{bmatrix} \mathbf{v}^{\text{R}} \\ \mathbf{v}^{\text{I}} \end{bmatrix}}_{\widetilde{\mathbf{v}}}, \tag{5}$$

where the superscripts 'R' and 'I' are used to represent a matrix whose elements are the real and imaginary parts, respectively, of the original matrix.

From (5), we can argue that the optimum estimator which estimates $\mathbf{s}$ from $\widetilde{\mathbf{y}}$ might be the minimum mean square error (MMSE) estimator. The MMSE estimator is optimum in a sense that it minimizes the norm of the error vector between the estimated values and the actual ones. However, implementation of the MMSE estimator requires a matrix inversion that makes it a complex estimation method, specially for large values of K. Interestingly, as it was suggested by [22], column vectors of the channel matrix are asymptotically orthogonal, i.e.,

$$\left(\widetilde{\mathbf{H}}^{\text{T}}\widetilde{\mathbf{H}}\right)_{N\gg K} \approx \mathbf{D}, \tag{6}$$

where $\mathbf{D}$ is a diagonal matrix. This suggests the matched filter (MF) as an alternative solution to the MMSE estimator. In the case of MF estimation, we can obtain the estimate of the vector $\mathbf{s}$ according to

$$\hat{\mathbf{s}} = \mathbf{\Gamma}\mathbf{D}^{-1}\widetilde{\mathbf{H}}^{\text{T}}\widetilde{\mathbf{y}}, \tag{7}$$

where $\mathbf{\Gamma}$ consists of the first K rows of the identity matrix $\mathbf{I}_{2K}$. Accordingly, by increasing the number of BS hydrophones, the performance of MF estimator approaches to the its MMSE counterpart, and the effect of multiuser interference and noise will vanish [2].

B. Self Equalization Property

One of the fundamental assumptions often made in the implementation of FBMC systems is that in each subchannel, the channel can be modeled by a flat gain, and the receiver can use a single tap equalizer at each subcarrier in order to remove the effect of the channel frequency selectivity. This assumption will be only valid if the number of subcarriers is large. However, increasing the number of subcarriers is not

a desirable solution in the time-varying UWA channels since this would increase the duration of the FBMC symbols, which will consequently increase the Doppler-induced intercarrier interference (ICI).

In the case of massive MIMO, the presence of a large number of receiving antennas/hydrophones and the use of matched filter estimators lead to a phenomenon know as *self equalization*, [23]. Self equalization averages out the frequency selectivity introduced by different channels at each subcarrier, hence, allow widening the bandwidth of each subcarrier band; equivalently, increasing the symbol rate in FBMC. At this point, it is worth mentioning that shortening the length of the symbols has many advantages in UWA communications. Specifically, it leads to (i) Lower sensitivity to channel variations; (ii) Higher spectrum efficiency since as the interval between one symbol to another is reduced, one can rely on blind channel tracking methods instead of scattered pilots for the purpose of equalization. This is the subject of Section V-C; (iii) Lower sensitivity to carrier frequency offset and Doppler scaling; (iv) Lower networking latency and delay.

C. Adaptive Channel Tracking

As mentioned above, incorporating a large number of hydrophones at the BS leads to FBMC symbols with shorter durations. When the interval between the symbols is reduced, the channel variation from a symbol to another is also decreased. This enables us to exploit blind channel tracking methods to track the channel variations, symbol-by-symbol. This, in turn, eliminates the need of using scattered pilots subcarriers among the data subcarriers, and ultimately leads to a more bandwidth efficient communication network. Moreover, as it is shown numerically in Section VI, the adaptive channel update enhances the signal-to-interference-plus-noise-ratio (SINR) of the output constellation, compared to the case of MF (or MMSE) estimators.

The adaptive equalization that is employed in this paper is the constant modulus algorithm (CMA) proposed by Godard [24]. CMA is one of the most popular blind adaptation algorithms. However, it suffers from the problem of phase ambiguity [25]. In an FBMC system, since the symbols are real-valued numbers, the amount of phase ambiguity is limited to 0 or π radians. Hence, the phase ambiguity problem may be avoided if the matched filter coefficient are initialized to a point closed to their optimum values.

The CMA algorithm is developed by minimizing the cost function

$$\xi = \mathbb{E}[(|\hat{s}_{n,k}(\ell)|^p - R)^2] \tag{8}$$

where $\mathbb{E}[\cdot]$ denotes expectation, $\hat{s}_{n,k}(\ell)$ is the equalizer output of the ℓ^{th} user at the (n,k) time-frequency point, p is an integer (usually set equal to 1 or 2), $R = \mathbb{E}[|s|^{2p}]/\mathbb{E}[|s|^p]$, and s is a random selection from the PAM symbols alphabet. A least mean square (LMS) like algorithm is then developed to adjust the single tap equalizers.

Each packet starts with a known sequence of CMT symbols as a preamble. The rest of the packet contains data symbols. The preamble is used to identify the channel amplitude (magnitude and phase) response at each subcarrier and at each receiver hydrophone. The identified channel gains at each subcarrier are used to form the initial coefficients of the MF receiver. The blind adaptation is run subsequently over the payload part of the packet.

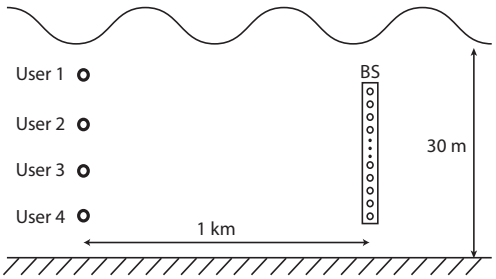

Fig. 3: Geometry of the simulation.

To put the above description in a mathematical form, assuming that $\mathbf{h}_\ell$ is estimated using the preamble at the receiver, the equalizer tap-weights, $\mathbf{w}_{n,k}(\ell)$, are initialized using the MF setting according to (7). The equalizer output is calculated as

$$\hat{s}_{n,k}(\ell) = \mathbf{w}_{n,k}^{\text{H}}(\ell)\mathbf{y}_{n,k}(\ell). \tag{9}$$

Once the MF combiner coefficients are initialized, an LMS-like blind tracking algorithm based on the cost function (8) is run to track the channel variation. Derivation of the relevant update equation is straightforward and can be derived following the same line of derivation as in [16]. The result is

$$\mathbf{w}_{n+1,k}(\ell) = \mathbf{w}_{n,k}(\ell) - 2\mu p(\text{sign}(\hat{s}_{n,k}(\ell)))^p(\hat{s}_{n,k}(\ell))^{p-1} \times(|\hat{s}_{n,k}(\ell)|^p - R)\mathbf{y}_{n,k}(\ell), \tag{10}$$

where μ is an step-size parameter.

VI. Numerical Results

In this section, we evaluate the performance of the proposed design using computer simulations. We use the Virtual Time-series EXperiment (VirTEX) underwater acoustic simulator, which has been developed recently [26]. VirTEX is a powerful package that runs on top of the BELLHOP ray tracing program [27], and computes the signal observed by the receiver, by taking into account the multipath and Doppler effects caused by the UWA environment.

Fig. 3 illustrates the geometry of our simulation. There are four transmitting users, which we assume are synchronized to transmit simultaneously. A multi-hydrophone BS resides at the receiver end. The users are transmitting CMT signals in a bandwidth of $B = 5$ kHz centered at the carrier frequency $f_c = 8$ kHz. In total, 32 subcarriers are considered in the transmission band. Hence each subcarrier has a bandwidth of $5000/32 \approx 150$ Hz. The symbol period is about 3 ms. Comparing this symbol period with those in previous works, e.g., [5], [6], one will find that this is an order of magnitude smaller. This choice, which was enabled thanks to a large number of BS hydrophones used in our system, facilitates the blind tracking of the channel variations as discussed in Section V-C.

Fig. 4 shows the estimated channel impulse response between user 2 and the top first BS hydrophone. We have set

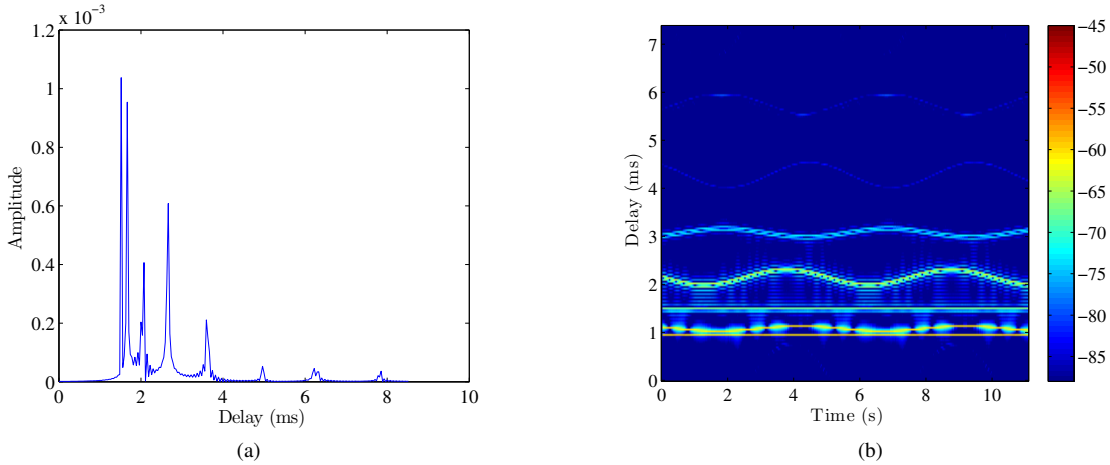

Fig. 4: (a) Estimated impulse response between the user 2 and the first hydrophone in the BS. (b) Variation of the channel impulse response (due to the gravity waves) over time for the same channel. The magnitude of the channel impulse response is presented in dB.

the parameters of the VirTEX simulator such that the simulated channel resembles a similar behavior to the typical at-sea channels that has been presented in UWA literature, e.g., Fig. 1 of [28].

The BS estimates the channel responses of the users through the preamble sequences, and the MF equalizer tap-weights are initialized according to (7). Subsequently, the BS adaptively tracks the channel using the CMA blind tracking algorithm. Fig. 6 illustrates the output binary PAM constellation of the detected symbols for the four users at the BS. Here, the BS consists of 40 receiving hydrophones. The detected data symbols from all subcarriers are included. SNR at the receiver front-end is 10 dB. A total of 8 bits of coded information per second per Hertz from four independent users are transmitted to the BS, simultaneously.

It is worth noting that the proposed system can tolerate some inaccuracy in the initial channel estimates (MF setting). The blind tracking algorithm subsequently improves on the MF estimator and results in an improvement in the detected symbols. This can be seen in Fig. 6. The tracking algorithm also remains stable as time passes and thus continuous data may be transmitted for a long time, without any need for pilots.

Fig. 5 shows the average SINR performance of the proposed design for different number of BS hydrophones. More receive hydrophones at the BS should result in a higher SINR performance. However, it should be noted that this behavior is only valid for a limited range of hydrophones. In fact, as we increase the number of hydrophones at the BS, the step-size parameter of the blind tracking algorithm (μ) should also be decreased to guarantee the convergence of the algorithm. This will in turn cause the tracking to be slower for larger array sizes.

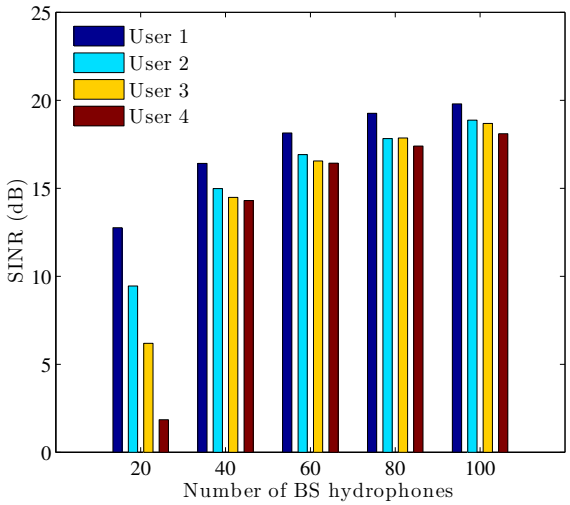

Fig. 5: SINR comparison of the proposed channel tracking algorithm for different number of BS hydrophones.

VII. Conclusion

This paper introduced the idea of Massive MIMO that has recently been proposed for 5G wireless communication systems as an attractive candidate for the UWA application. Moreover, the use of cosine modulated muticarrier/multitone (CMT) technique with its blind channel equalization capability was introduced in the proposed (Massive MIMO) setup to allow channel tracking without any need for pilot symbols, hence, a significant boost to bandwidth efficiency. Through computer simulations, we showed that the Massive MIMO setup will allow multiple terminals to transmit simultaneously to a base station/fusion center.

References

[1] D. Gesbert, M. Kountouris, R. W. Heath Jr, C.-B. Chae, and T. Sälzer, "Shifting the mimo paradigm," *Signal Processing Magazine, IEEE*, vol. 24, no. 5, pp. 36–46, 2007.

[2] T. Marzetta, "Noncooperative cellular wireless with unlimited numbers of base station antennas," *IEEE Transactions on Wireless Communications*, vol. 9, no. 11, pp. 3590–3600, 2010.

[3] F. Boccardi, R. W. Heath, A. Lozano, T. L. Marzetta, and P. Popovski, "Five disruptive technology directions for 5g," *Communications Magazine, IEEE*, vol. 52, no. 2, pp. 74–80, 2014.

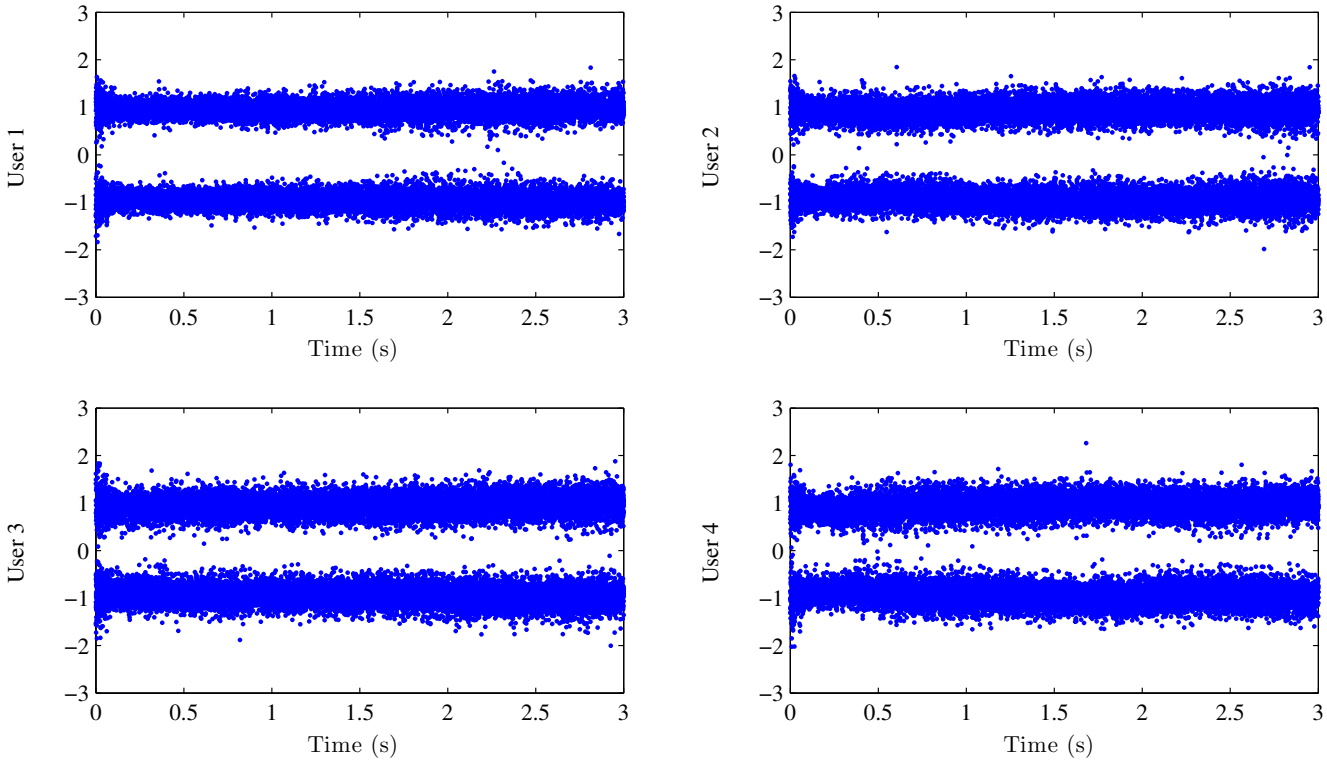

Fig. 6: Binary PAM constellation of the detected symbols at the BS, which consists of 40 receiving hydrophones.

[4] M. Stojanovic and J. Preisig, "Underwater acoustic communication channels: Propagation models and statistical characterization," *Communications Magazine, IEEE*, vol. 47, no. 1, pp. 84–89, 2009.

[5] P. Amini, R.-R. Chen, and B. Farhang-Boroujeny, "Filterbank multicarrier communications for underwater acoustic channels," *Oceanic Engineering, IEEE Journal of*, vol. PP, no. 99, pp. 1–16, 2014.

[6] B. Li, J. Huang, S. Zhou, K. Ball, M. Stojanovic, L. Freitag, and P. Willett, "Mimo-ofdm for high-rate underwater acoustic communications," *Oceanic Engineering, IEEE Journal of*, vol. 34, no. 4, pp. 634–644, 2009.

[7] R. Chang, "High-speed multichannel data transmission with bandlimited orthogonal signals," *Bell Sys. Tech. J.*, vol. 45, pp. 1775–1796, Dec. 1966.

[8] B. Saltzberg, "Performance of an efficient parallel data transmission system," *IEEE Transactions on Communication Technology*, vol. 15, no. 6, pp. 805–811, 1967.

[9] B. Hirosaki, "An orthogonally multiplexed qam system using the discrete fourier transform," *IEEE Transactions on Communications*, vol. 29, no. 7, pp. 982–989, 1981.

[10] H. Bölcskei, "Orthogonal frequency division multiplexing based on offset QAM," *Advances in Gabor Analysis*, pp. 321–352, 2003.

[11] B. Hirosaki, S. Hasegawa, and A. Sabato, "Advanced groupband data modem using orthogonally multiplexed qam technique," *IEEE Transactions on Communications*, vol. 34, no. 6, pp. 587–592, 1986.

[12] P. Siohan, C. Siclet, and N. Lacaille, "Analysis and design of ofdm/oqam systems based on filterbank theory," *IEEE Transactions on Signal Processing*, vol. 50, no. 5, pp. 1170–1183, 2002.

[13] P. Vaidyanathan, *Multirate Systems and Filter Banks*. Englewood Cliffs, New Jersey, Prentice Hall, 1993.

[14] M. Tzannes, M. Tzannes, and H. Resnikoff, "The dwmt: A multicarrier transceiver for adsl using m-band wavelet transforms," *ANSI Contribution T1E1.4/93-067*, March 1993.

[15] S. Sandberg and M. Tzannes, "Overlapped discrete multitone modulation for high speed copper wire communications," *IEEE Journal on Selected Areas in Communications*, vol. 13, no. 9, pp. 1571–1585, 1995.

[16] B. Farhang-Boroujeny, "Multicarrier modulation with blind detection capability using cosine modulated filter banks," *IEEE Transactions on Communications*, vol. 51, no. 12, pp. 2057–2070, 2003.

[17] L. Lin and B. Farhang-Boroujeny, "Cosine modulated multitone for very high-speed digital subscriber lines," *EURASIP Journal on Applied Signal Processing*, vol. 2006, p. 16 pages, 2006.

[18] B. Farhang-Boroujeny and C. (George) Yuen, "Cosine modulated and offset qam filter bank multicarrier techniques: a continuous-time prospect," *EURASIP Journal on Applied Signal Processing, 2010, special issue on Filter Banks for Next Generation Multicarrier Wireless Communications*, vol. 2010, p. 16 pages, 2010.

[19] A. Aminjavaheri, A. Farhang, A. RezazadehReyhani, and B. Farhang-Boroujeny, "Impact of timing and frequency offsets on multicarrier waveform candidates for 5G," in *2015 IEEE Signal Processing Workshop (SPW2015)*, Salt Lake City, USA, Aug. 2015, pp. 372–377.

[20] B. Farhang-Boroujeny, "OFDM Versus Filter Bank Multicarrier," *IEEE Signal Processing Magazine*, vol. 28, no. 3, pp. 92–112, 2011.

[21] D. Katselis, E. Kofidis, A. Rontogiannis, and S. Theodoridis, "Preamble-based channel estimation for cp-ofdm and ofdm/oqam systems: A comparative study," *Signal Processing, IEEE Transactions on*, vol. 58, no. 5, pp. 2911–2916, 2010.

[22] F. Rusek, D. Persson, B. K. Lau, E. G. Larsson, T. L. Marzetta, O. Edfors, and F. Tufvesson, "Scaling up mimo: Opportunities and challenges with very large arrays," *Signal Processing Magazine, IEEE*, vol. 30, no. 1, pp. 40–60, 2013.

[23] A. Farhang, N. Marchetti, L. Doyle, and B. Farhang-Boroujeny, "Filter bank multicarrier for massive MIMO," in *arXiv: 1402.5881, to appear in the proceedings of VTC Fall*, 2014.

[24] D. Godard, "Self-recovering equalization and carrier tracking in two-dimensional data communication systems," *IEEE Transactions on Communications*, vol. 28, p. 11, 1980.

[25] R. Johnson, P. Schniter, T. J. Endres, J. D. Behm, D. R. Brown, and R. A. Casas, "Blind equalization using the constant modulus criterion: A review," *Proceedings of the IEEE*, vol. 86, no. 10, pp. 1927–1950, 1998.

[26] J. C. Peterson and M. B. Porter, "Virtual timeseries experiment (virtex)–quick start," *http://oalib.hlsresearch.com/Rays/VirTEX/README.pdf*, 2011.

[27] M. Porter, "Bellhop gaussian beam/finite element beam code," *Available in the Acoustics Toolbox, http://oalib. hlsresearch. com/Rays*, 2007.

[28] W. Li and J. C. Preisig, "Estimation of rapidly time-varying sparse channels," *Oceanic Engineering, IEEE Journal of*, vol. 32, no. 4, pp. 927–939, 2007.